УДК 539.172.17

PRODUCTION OF NUCLEI IN ^{32,34,36}S-INDUCED REACTIONS IN THE ENERGY RANGE 6 ÷ 75 MeV/A

***O.B.Tarasov*[1], *Yu.E.Penionzhkevich*[1], *R.Anne*[2], *D.S.Baiborodin*[1], *D.Guillemaud-Mueller*[3], *A.S.Fomichev*[1], *R.Kalpakchieva*[1], *M.Lewitowicz*[2], *S.M.Lukyanov*[1], *V.Z.Maidikov*[1], *A.C.Mueller*[3], *Yu.Ts.Oganessian*[1], *M.G.Saint-Laurent*[2], *N.K.Skobelev*[1], *O.Sorlin*[3], *V.D.Toneev*[4], *W.Trinder*[2]**

Some regularities in the production of isotopes with $6 \le Z \le 14$ are investigated in reactions induced by ^{32,34,36}S beams at $6 < E < 75$ MeV/A on targets of ^{nat}C, ^{181}Ta and ^{197}Au. The isotope yields and the most probable fragment mass A (for a given Z) are studied as a function of target, projectile mass and energy. A comparison is made of the experimental data at low energies with calculations in the framework of the dynamical model of deep inelastic collisions. The obtained data are considered from the point of view of the feasibility of heavy ion beams for producing nuclei far from the line of stability.

The investigation has been performed at the Flerov Laboratory of Nuclear Reactions, JINR, and at GANIL (France).

Образование ядер в реакциях с ионами ^{32,34,36}S в диапазоне энергий 6 ÷ 75 МэВ/А

О.Б.Тарасов и др.

В настоящей работе исследуются закономерности образования различных изотопов элементов с $6 \le Z \le 14$ в реакциях на пучках ^{32,34,36}S в диапазоне энергий $6 \le E \le 75$ МэВ/А. Получены выходы ядер в зависимости от мишени, от энергии пучка и от нейтронного избытка ядер пучка. На основе экспериментальной информации даны оценки образования различных изотопов для промежуточных энергий на пучках ^{32,34,36}S. Приведены сравнения экспериментальных результатов в области низких энергий с расчетами по динамической модели глубоконеупругих столкновений. Полученные данные обсуждаются с точки зрения возможностей реакций с тяжелыми ионами в широком диапазоне энергий для получения ядер, удаленных от линии стабильности.

Работа выполнена в Лаборатории ядерных реакций им.Г.Н.Флерова ОИЯИ и в ГАНИЛ (Франция).

[1]Flerov Laboratory of Nuclear Reactions, JINR, Dubna.
[2]Grand Accelerateur National d'Ions Lourds, Caen, France.
[3]Institut de Physique Nucleaire, Orsay, France.
[4]Bogoliubov Laboratory of Theoretical Physics, JINR, Dubna.

1. Introduction

Heavy-ion induced reactions are shown to be one of the most efficient tools for producing nuclei far from the stability line. The first experiments carried out in Dubna using ^{22}Ne and ^{40}Ar beams of 7 MeV/A resulted in the observation of about 20 new isotopes lying significantly away from stability [1,2]. In these experiments, a new heavy-ion-reaction mechanism was discovered which later on was called deep inelastic reactions [2]. This process, corresponding to a transitional regime between complete fusion and direct reactions, has been well studied at energies up to 10 MeV/A. It was shown that in deep inelastic processes the production yields of different isotopes could be well described using statistical models [3], and could also be explained by the reaction Q-value taking into account pairing corrections (Q_{gg}-systematics) [2]. However, the advent to the region of nuclear instability by using deep inelastic reactions was limited by the low production cross sections of the sought-after exotic nuclear species. Later, reactions with high-energy heavy ions were used, where as a result of the projectile fragmentation on a thick target many new neutron-rich light-element isotopes were produced with relatively high cross sections [4]. The advent into the region of more neutron-rich isotopes and of heavier elements required beams of heavy projectiles with higher intensities. In the late 1970s, the availability of new heavy ion accelerators of intermediate energies provided further possibilities of using reactions induced by heavy ion beams of $E = 50 \div 100$ MeV/A for the production of new exotic nuclei. Very successful was proven to be the use of ^{36}S and ^{48}Ca beams in the fragmentation of which many extremely neutron-rich nuclei were observed. A series of experiments using a ^{48}Ca beam, performed within the GANIL-Dubna collaboration, made possible the observation and investigation of the properties of over 20 new isotopes lying close to the limit of particle stability [5]. There is evidence that, although for a certain domain of nuclei the fragmentation process is dominant already at 27 MeV/A [6], the multinucleon transfer reaction plays still a noticeable role. For example, in ^{58}Ni($Z = 28$)-induced reactions at 55 MeV/A new neutron-deficient Cu isotopes were observed [7]. A similar effect, viz. production of charge pickup products ($Z > 50$), has been observed also in ^{112}Sn-induced reaction at 63 MeV/A [8]. The continuous investigation of the mechamism of nuclear reactions is closely connected with the projects for radioactive nuclear beam facilities, which will open new possibilities for the study of exotic nuclei and where, for the generation of radioactive secondary beams, primary beams of very different energies will be used [9], e.g. 100 MeV/A (GANIL), 20 MeV/A (Dubna) and up to 1 GeA/A (GSI and RIKEN). Questions arise concerning the extent of coexistence of different reaction mechanisms (e.g., multinucleon transfer reactions and fragmentation) at various energies, the dependence of the production rates on the projectile and target isospin, etc.

The present work was undertaken in order to obtain experimental information on the trends in the formation of different isotopes with $6 \leq Z \leq 14$ in reactions induced by ^{32,34,36}S beams in the energy range $6 < E < 75$ MeV/A.

2. Experimental Procedure

The experiments with $^{32,34}S$ beams of energies $6 < E < 20$ MeV/A were carried out at the U400 cyclotron of the Flerov Laboratory of Nuclear Reactions (JINR). The yields of the various isotopes were measured at a laboratory angle $\theta_{lab} = 4°$ using the MSP-144 magnetic spectrometer [10] with a position-sensitive ionization chamber as the focal plane detector [11]. The solid angle was 0.85 msr; and the momentum acceptance, ± 4.1%. In the measurements, targets of ^{nat}C (400 μg/cm^2 thick) and ^{197}Au (200 μg/cm^2 thick) were used. The beam monitoring was performed by means of a Faraday cup. The Z and A identification of the reaction products was done using the measured energy-loss (dE), total energy (E) and position (x) in the focal plane. The relations used are:

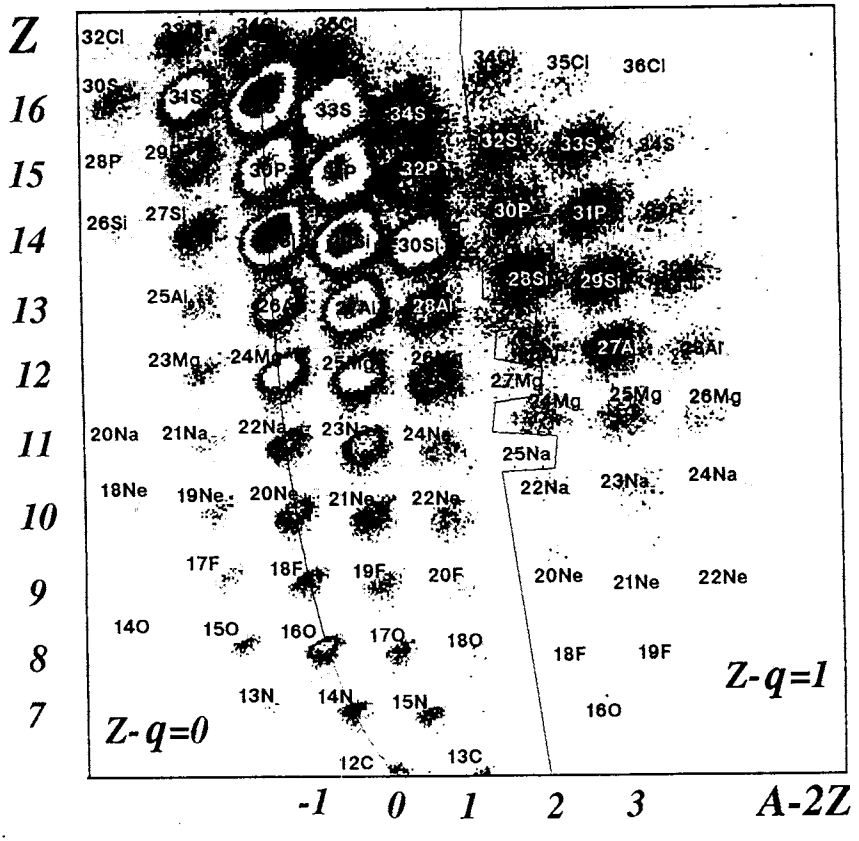

Fig.1. Identification matrix ($A - 2Z$, Z) of the products of the ^{32}S (14.5 MeV/A) + C reaction obtained at a magnetic field $B = 0.7975$ T. The left solid line passes through the completely stripped nuclei with zero isotopic spin. The right curve discriminates between regions of nuclei with charge $q = Z$ and $q = Z - 1$

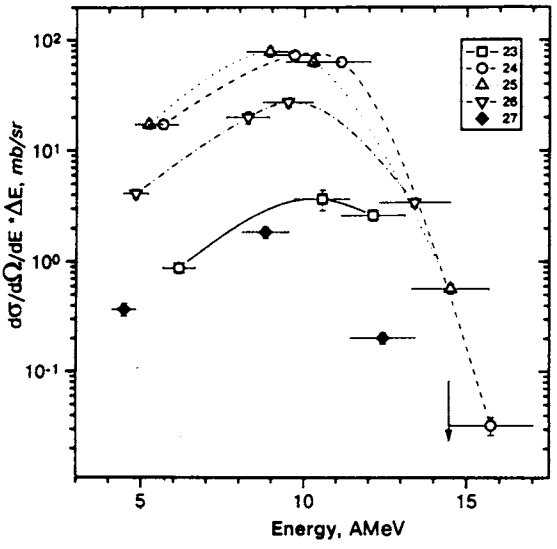

Fig.2. Energy spectra of magnesium isotopes from the reaction ^{32}S (14.5 MeV/A) + C. The horizontal error bars indicate the energy acceptance at the corresponding magnetic rigidity of the spectrometer. The vertical arrow indicates the primary beam energy. The curves are the result of smoothing

$$dE \approx \frac{AZ^2}{E}, \tag{1}$$

$$E = K(Bx)^2 \frac{q^2}{A}, \tag{2}$$

where A, Z and q are the mass, the atomic number and the ionic charge of the nucleus, respectively, B — the magnetic field of the spectrometer and k — a constant. For a better presentation of the identified isotopes a two-dimensional plot of production yields as a function of $A - 2Z$ and Z was used. One example is shown in Fig.1. As can be seen from the figure, in the given experimental set-up, a good separation of the isotopes ranging from C to Cl was achieved, which in turn allowed unambiguous identification of the reaction products.

Several settings of magnetic spectrometer was used in order to obtain the energy spectra of the produced isotopes. Fig.2 represents the energy distributions of Mg isotopes obtained in the reaction ^{32}S (14.5 MeV/A) + C.

The ^{36}S (75 MeV/A)-beam was provided by the accelerator complex GANIL (France) and the isotope yields were measured [12] with the help of the fragment separator LISE [13].

3. Experimental Results and Their Analysis

The results discussed in the present work have been obtained in reactions induced by $^{32,34,36}S$ ions in a very broad energy range.

The distributions of carbon, oxygen, neon, magnesium and silicon isotopes produced in the ^{36}S (75 MeV/A)-projectile fragmentation on two targets (^{nat}C and ^{181}Ta) are shown in Fig.3. To describe the experimental data on the production cross sections of the isotopes

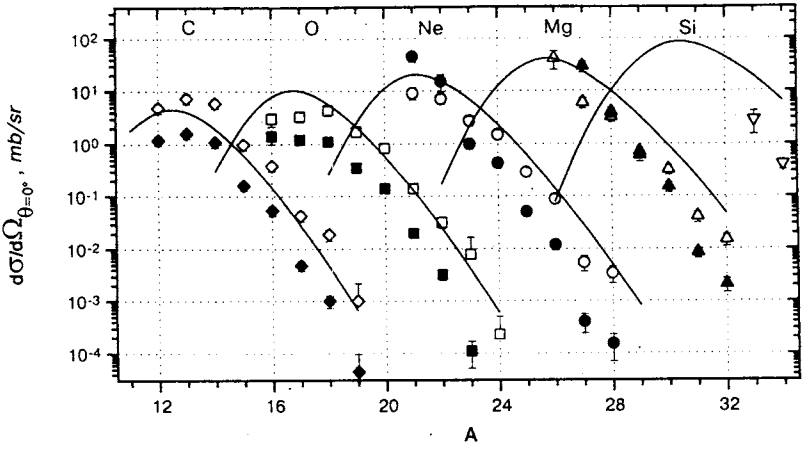

Fig.3. Experimental isotopic distributions of carbon, oxygen, neon, magnesium and silicon nuclei obtained in the fragmentation of a 75 MeV/A ^{36}S beam on two targets — ^{12}C (closed symbols) and ^{181}Ta (open symbols) [12]. The solid line is the result of calculations for the Ta target based on a modification of the empirical parameterization [14]

with atomic nubmers $6 \leq Z \leq 14$ an empirical parametrization similar to the one in [14] was used. The calculations for the Ta-target, denoted by the solid line in Fig.3, show a satisfactory agreement with the experimental data. It can also be seen that at an energy of 75 MeV/A the production cross sections of neutron-rich nuclei are higher for the Ta than for the C-target.

Figures 4a,b show the experimental isotopic distributions from the ^{32}S (9.1 and 16.1 MeV/A) beam for two target (^{nat}C and ^{197}Au), and Fig.4c — the calculations for ^{32}S at 75 MeV/A, obtained as for Fig.3 using the same set of parameters. From the comparison of the experimental data with the calculations it follows that the isotopic distributions can be described by a smooth curve close to a Gaussian distribution. The widths of these distributions at 9.1 and 16.1 MeV/A differ strongly for the two targets (^{nat}C, ^{197}Au), at least for the isotopes of elements far from the projectile (oxygen and neon). At the same time, the yield of the neutron-rich isotopes of these elements in the case of the Au-target is significantly higher than in the case of the C-target.

The comparison (Fig.5) of the differential production cross sections as a function of the atomic number Z of the products for different targets, projectile energies and projectile neutron excess has made it possible to draw the following conclusions about the trends in the formation of various nuclei in S-induced reactions.

At energies 7 ÷ 10 MeV/A for the light target, a rather large drop in cross section for smaller Z-values (or greater number of transferred protons) is observed: from 700 mb/sr, in the case of two stripped protons, to 1 mb/sr, for the stripping of 7 protons (see Fig.5a). At higher bombarding energies this difference decreases and at intermediate energies is negligible (Fig.5b). Comparison of reactions induced by projectiles of different mass shows that

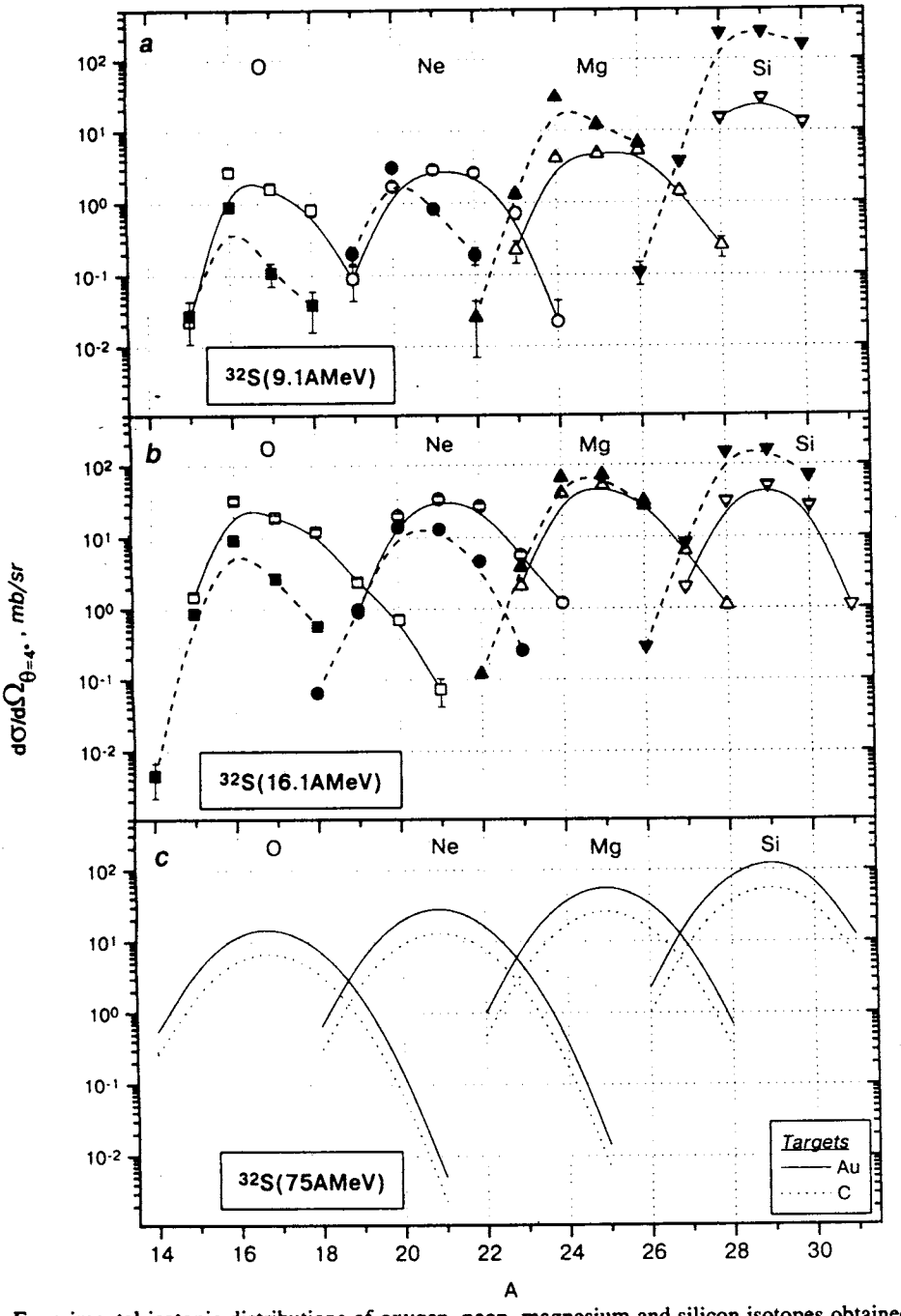

Fig.4. Experimental isotopic distributions of oxygen, neon, magnesium and silicon isotopes obtained for two targets, ^{12}C (closed symbols) and ^{197}Au (open symbols), at a laboratory angle $\theta_{lab} = 4°$ and at two different energies of ^{32}S, 9.1 MeV/A (a), and 16.1 MeV/A (b). Calculated distributions for 75 MeV/A are presented for $\theta_{lab} = 0°$ in (c). The curves on (a) and (b) are the result of smoothing

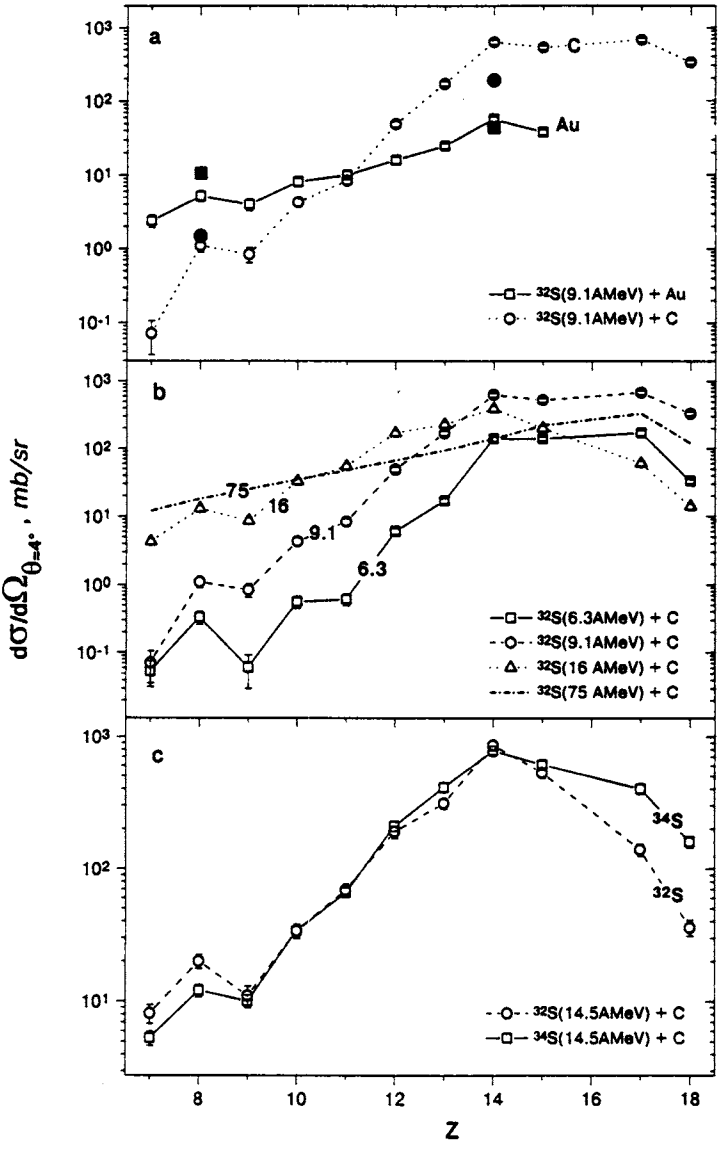

Fig.5. Differential production cross sections of elements vs the atomic number Z. Comparisons are made for: (a) different targets for the ^{32}S beam (9.1 MeV/A), (b) different incident energies of the ^{32}S beam on the C-target, (c) different neutron excesses of the projectile in the case of ^{32}S (14.5 MeV/A) and ^{34}S (14.6 MeV/A) beams. The closed symbols in (a) correspond to theoretical calculations carried out in the framework of the dynamical model of deep inelastic collisions [17]

the cross sections obtained for ^{32}S and ^{34}S beams are very close to each other. Significant difference can be noticed only for products with Z higher than the projectile atomic number, which corresponds to the case of pick-up of protons by the projectile (Fig.5c).

A comparison of the centers of gravity of the isotopic differential-cross-section-distribuions of Fig.4, corresponding to neutron excess values (N–Z), is shown in Fig.6 for the studied reactions as a function of the atomic number Z. In the case of the heavy target, one can observe on the average a shift of the centers of gravity in the direction of the neutron-rich region when decreasing the bombarding energy (Fig.6a). On the contrary, the displacement is towards the proton-rich side for the light target (Fig.6b). The observed trend is in a qualitative agreement with the microscopic theory of multinucleon exchange [15]. The direction of the flow of nucleons in the system is determined by the difference in the corresponding Fermi energies, with the nucleons «flowing» from the nucleus with a higher Fermi energy to the nucleus with the smaller one. The decreased shift in the centers of gravity with increasing the projectile energy in the case of the heavy target can be explained by the high excitation, which can lead to the emission of a larger number of neutrons. Moreover, at small incident energies oscillations are observed in the centers-of-gravity distributions, due to odd-even effects, which are smoothed with increasing the energy. Figures 6c,d show the Z dependence of the most probable neutron excess of the produced isotopes for the two ion beams, ^{32}S and ^{34}S, at an energy of 14.5 MeV/A (experimental data) and at 75 MeV/A (calculated values). From Fig.6c it follows that, from the point of view of the production of neutron-rich isotopes, there is only a small advantage in using a ^{34}S beam compared to a beam of ^{32}S at an energy of 14.5 MeV/A. However, at high energies some advantage can be expected, but only for the production of nuclei close to the projectile with $Z \geq 12$.

As it was mentioned earlier, the yields of isotopes in deep inelastic processes are well described by the reaction energy (Q_{gg}). The cross sections are determined by the relation [2]:

$$\sigma \sim \exp\{[Q_{gg} + \Delta E_c - \delta]/T\}, \tag{3}$$

where Q_{gg} is the energy necessary for the rearrangement of the nuclei in the input channel into the nuclei in the exit channel, ΔE_c — the change in the Coulomb energy of the system due to the redistribution of protons between the nuclei and to the deformation of the system, δ — the nucleon pairing corrections, and T — the temperature of the dinuclear system. Figure 7 presents the experimental differential cross sections for producing oxygen isotopes as a function of Q_{gg} for different target-projectile combinations at various projectile energies. It can be seen that there is an overall good agreement between the experimental points and the expected from relation (3). Making use of the Q_{gg} systematics, it is possible to estimate the yields of nuclei lying far from the stability line.

The obtained experimental results are of great interest from the point of view of the reaction mechanism involved in the formation of nuclei and because they give a possibility of estimating the usefulness of heavy-ion-induced reactions as a way to produce high-intensity beams in radioactive nuclear beam factories. For this purpose it is necessary to

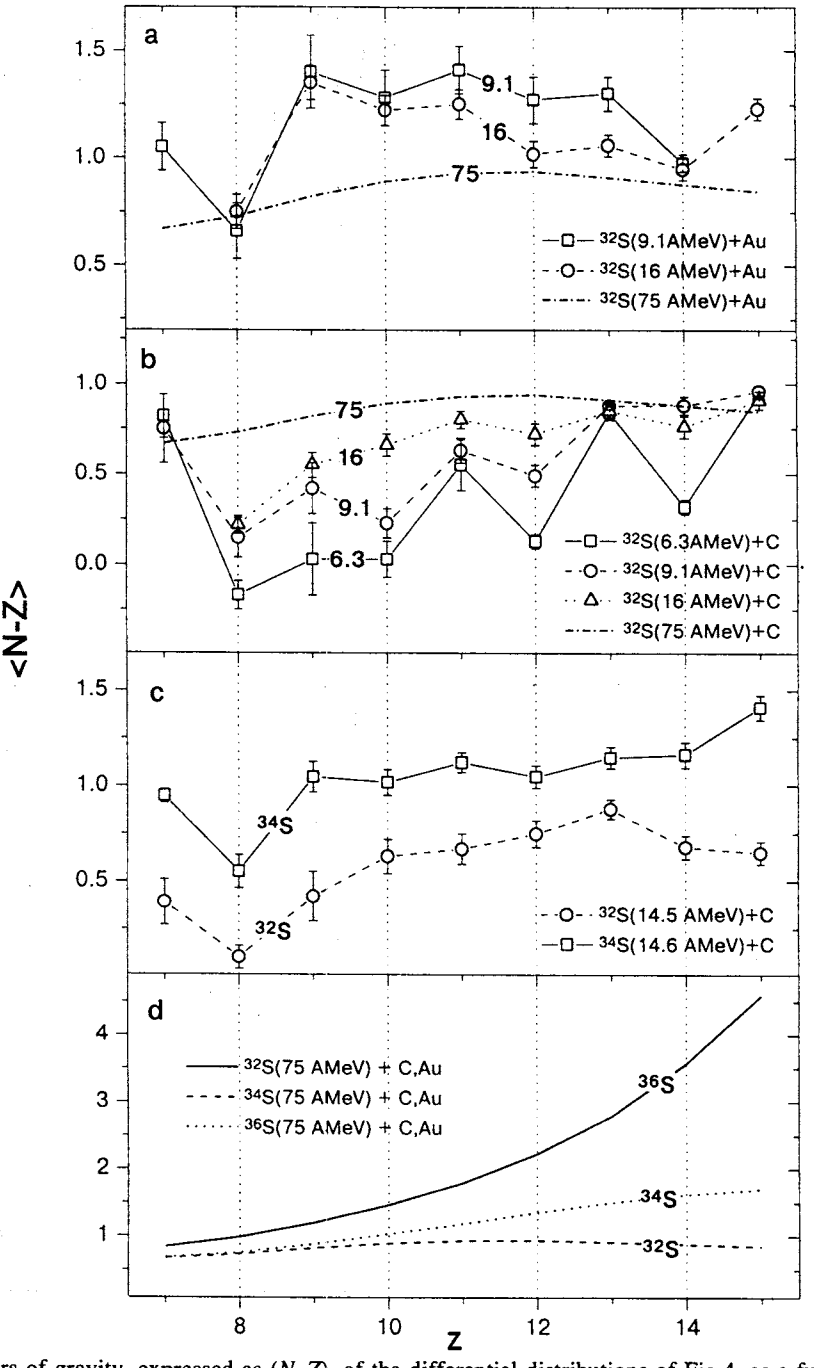

Fig.6. Centers of gravity, expressed as (*N–Z*), of the differential distributions of Fig.4, as a function of the atomic number Z. Energy dependence for the ^{32}S beam for the gold target (a), the carbon target (b); dependence on the projectile neutron excess at an energy of 14.5 MeV/A for a carbon target (c), and calculations for ^{32,34,36}S at 75 MeV/A (d)

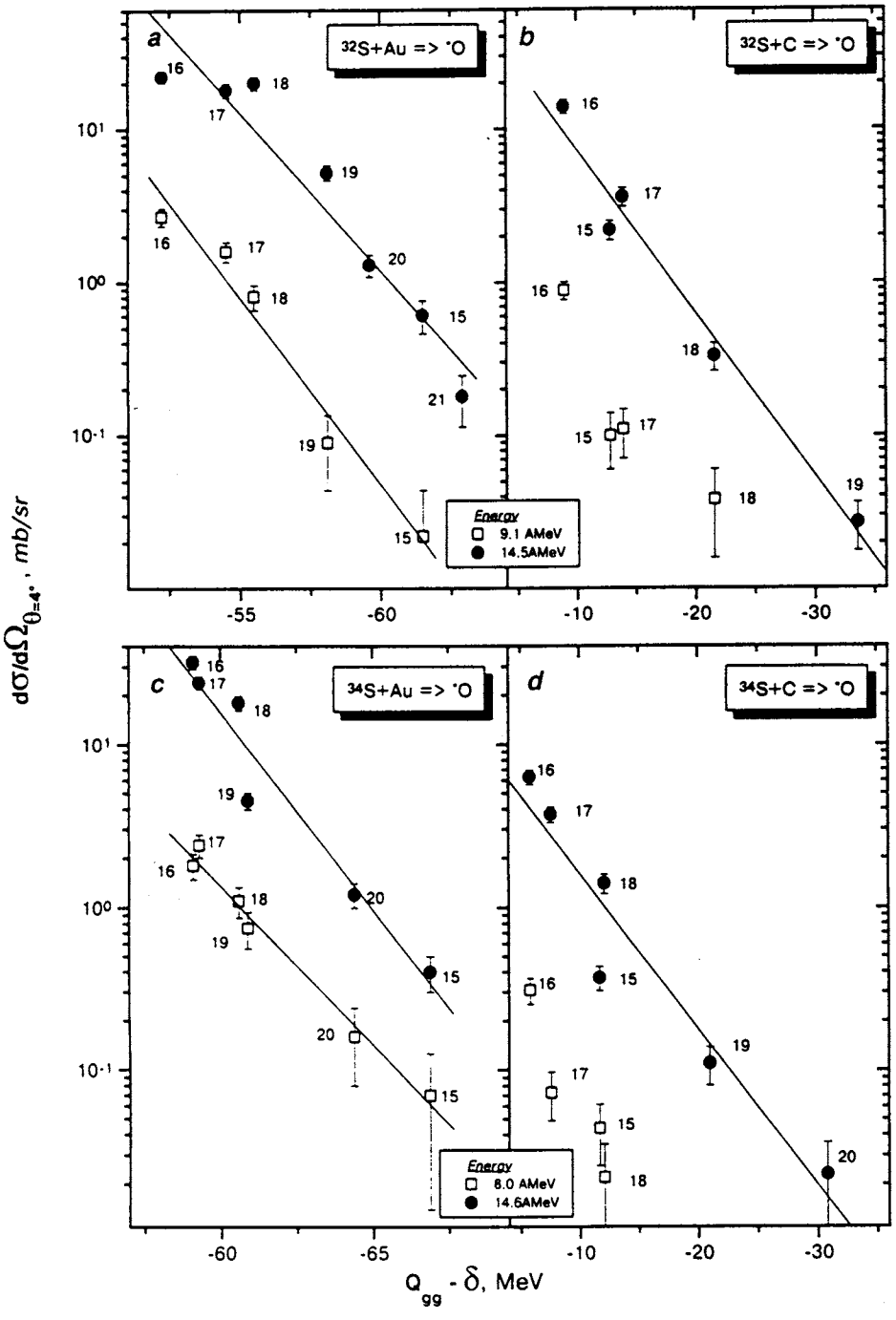

Fig.7. Experimental differential production cross sections for oxygen isotopes as a function of Q_{gg}, in different target-projectile combinations at various energies. The lines are fits with the relation $d\sigma / d\Omega = C_1 \exp [C_2(Q_{gg} - \delta)]$

consider the total reaction cross sections, which means that the angular distributions of the products have to be taken into account.

The angular distributions at low energies $6 < E < 20$ MeV/A were calculated in the framework of the dynamical model of deep inelastic collisions [16,17]. This model takes into account both the dissipation of the kinetic energy of the colliding nuclei and the fluctuations of the motion of the nuclei with respect to the classical trajectories, as well as the effect of deformation of the fragments in the exit channel. The results of the calculations for producing oxygen nuclei in the $^{32}S + ^{197}A$ reaction are presented in Fig.8. The solid and dashed curves correspond to deep inelastic fragments produced at different ion kinetic energy losses ($\Delta E > 50$ MeV and $\Delta E > E - V_C$). In Fig.8, two experimental points from the present experiment are also included. They are in agreement with the calculation corresponding to the small kinetic energy losses. This implies that the differential cross sections can be transformed to total cross sections by integrating over the angular distributions for the small kinetic energy losses.

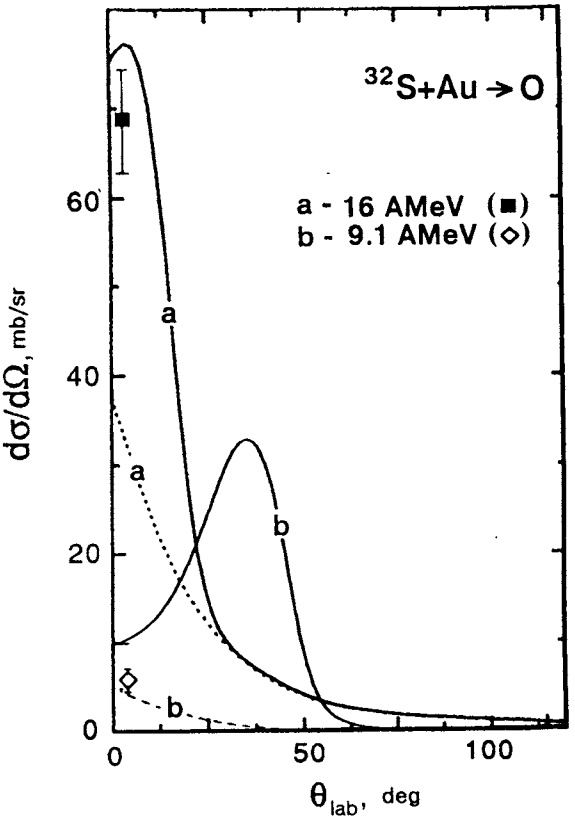

Fig.8. Angular distributions for oxygen isotopes obtained in the reaction $^{32}S + Au$ at 16 MeV/A (a) and 9.1 MeV/A (b), calculated in the framework of the dynamical model of deep inelastic collisons [17]. The solid and dashed curves correspond to deep inelastic fragments produced at projectile kinetic energy losses $\Delta E > 50$ MeV and $\Delta E > E - V_C$. The two points are from the present experiment

In the intermediate energy domain, the maximum of the angular distribution of the reaction products lies at $\theta \cong 0°$. The transformation of the differential into total cross sections was made on the basis of the angular distributions calculated by the method used in Ref.18. In the laboratory coordinate system, the angular distributions of products at intermediate energies can be described according to [18] by the expressions:

$$\frac{d^2\sigma}{d\Omega\, dE_A} \propto \sqrt{2AE_A}\, \exp\left[-\frac{A}{\sigma_P^2}\left(E_A - 2\cos\theta \sqrt{E_A \bar{E}} \right) + \bar{E} \right], \qquad (4)$$

where A and E_A are the mass number and the kinetic energy of the fragment, respectively, $\overline{E}$ is the most probable value of the energy and σ_p is the width of the fragment momentum distribution.

The total production cross sections for some isotopes of oxygen obtained by integrating over the angular distributions are shown in Fig.9 as a function of the energy of the projectiles ^{32,34,36}S. As can be seen from Fig.9a the cross sections rise for incident energies up to 15 + 20 MeV/A. For higher energies it can be speculated that they either go to a plateau (^{15}O) or pass through a maximum, after which they tend to decrease (^{19}O, ^{21}O). The solid curves in the figure are the results of smoothing. The dashed lines present the calculated cross sections of transfer reaction products (normalized to the experimental points) as a function of projectile energy. The calculation of the yields of the primary fragments was carried out using the microscopic transport model assuming a binary character of the reaction [15]. The isotopic distributions of the final (experimentally observed) nuclei were calculated within the framework of the statistical theory of decay of excited primary fragments [19].

The comparison of the experimental data and the calculations shows (see Fig.9a) that the contribution from deep inelastic transfer reactions to the cross section of producing both neutron-rich and neutron-deficient isotopes is dominant at low energies, while at intermediate energies the main contribution comes from fragmentation reactions. Nevertheless, as one can see from the figure, at intermediate energies the contribution of multinucleon transfer reactions is still noticeable.

On the basis of the experimental data shown in Fig.9, the yields of different oxygen isotopes as a function of projectile energy were calculated, assuming total absorption in the target of the beam having an initial energy E_0, using the relation:

$$N(E_0) = \int_{V_C}^{E_0} \frac{\sigma(E) N_{\text{beam}}}{M_{\text{target}}} \left(\frac{dE}{dX} \right)^{-1} dE \quad [\text{sec}^{-1}], \tag{5}$$

where V_C is the Coulomb barrier, $\sigma(E)$ — the cross section in units of [cm^2], N_{beam} — the intensity of the beam [pps], M_{target} — the mass of the target nucleus in [mg] and dE/dX corresponds to the stopping power of the projectiles in the target [MeV/(mg/cm^2)]. The yields of oxygen isotopes, calculated using the expession (S), produced in S-induced reaction on a gold target at a beam intensity of 1 eμA are presented in Fig.10 as a function of the projectile energy. In the upper panel (a) one can see the yields of ^{15}O, ^{19}O, and ^{21}O produced by a ^{32}S beam, while in the lower panel (b), the yields of the isotope ^{21}O produced using beams of ^{32}S, ^{34}S, and ^{36}S. From Fig.10a it follows that an increase in the projectile energy leads to an abrupt rise in the yield of neutron-deficient nuclei (^{15}O), while the increase in the yield of neutron-rich nuclei (^{21}O) is negligible. In Fig.10b, it can be seen that at energies of up to 20 MeV/A the difference between the yields of ^{21}O produced with different beams is small. At 75 MeV/A this difference increases and amounts to an order of magnitude for the ^{32}S and ^{36}S beams.

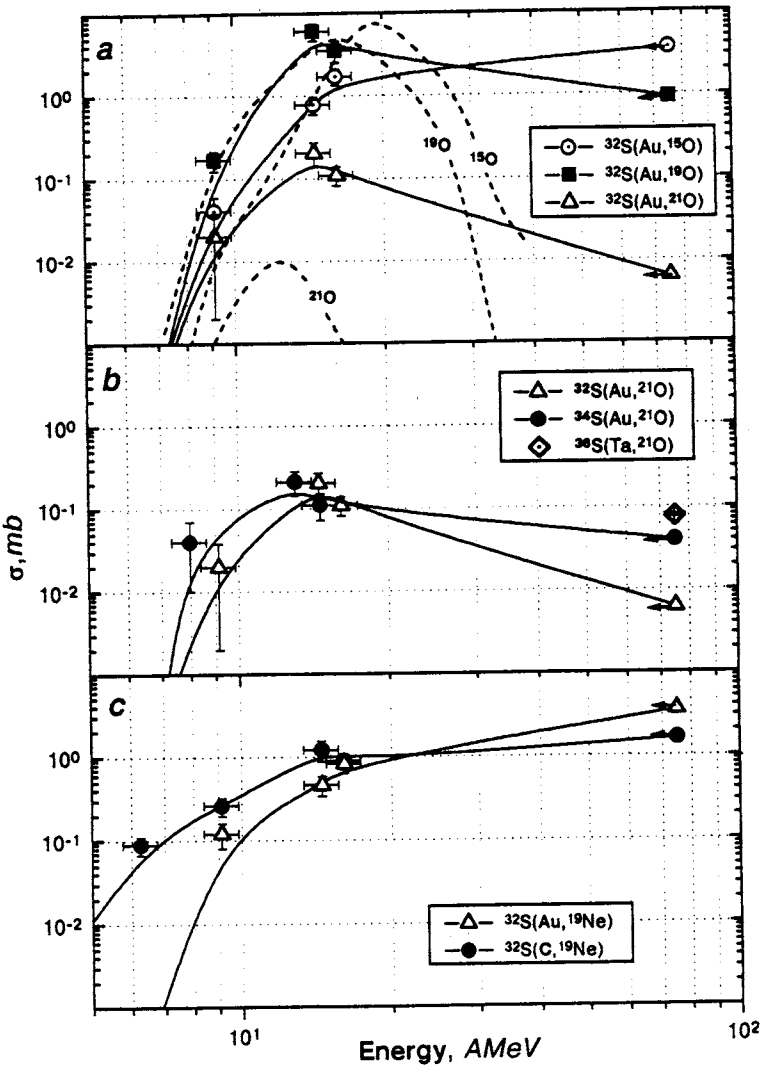

Fig.9. Total production cross sections for different isotopes as a function of energy. Cross sections for producing of: (a) oxygen isotopes in the irradiation of a gold target by the ^{32}S beam; (b) ^{21}O on a gold target by projectiles of different neutron excess, including an experimental point at 75 MeV/A for the ^{36}S-beam; (c) ^{19}Ne on different targets by the ^{32}S-beam. The cross sections for ^{32,34}S (75 MeV/A)-fragmentation were calculated using a modification of the empirical parameterization [14] and are denoted by arrows. The solid curves in the figure are the results of smoothing. The dashed lines present the calculated cross sections of transfer reaction products (normalized to ^{19}O) as a function of the projectile energy

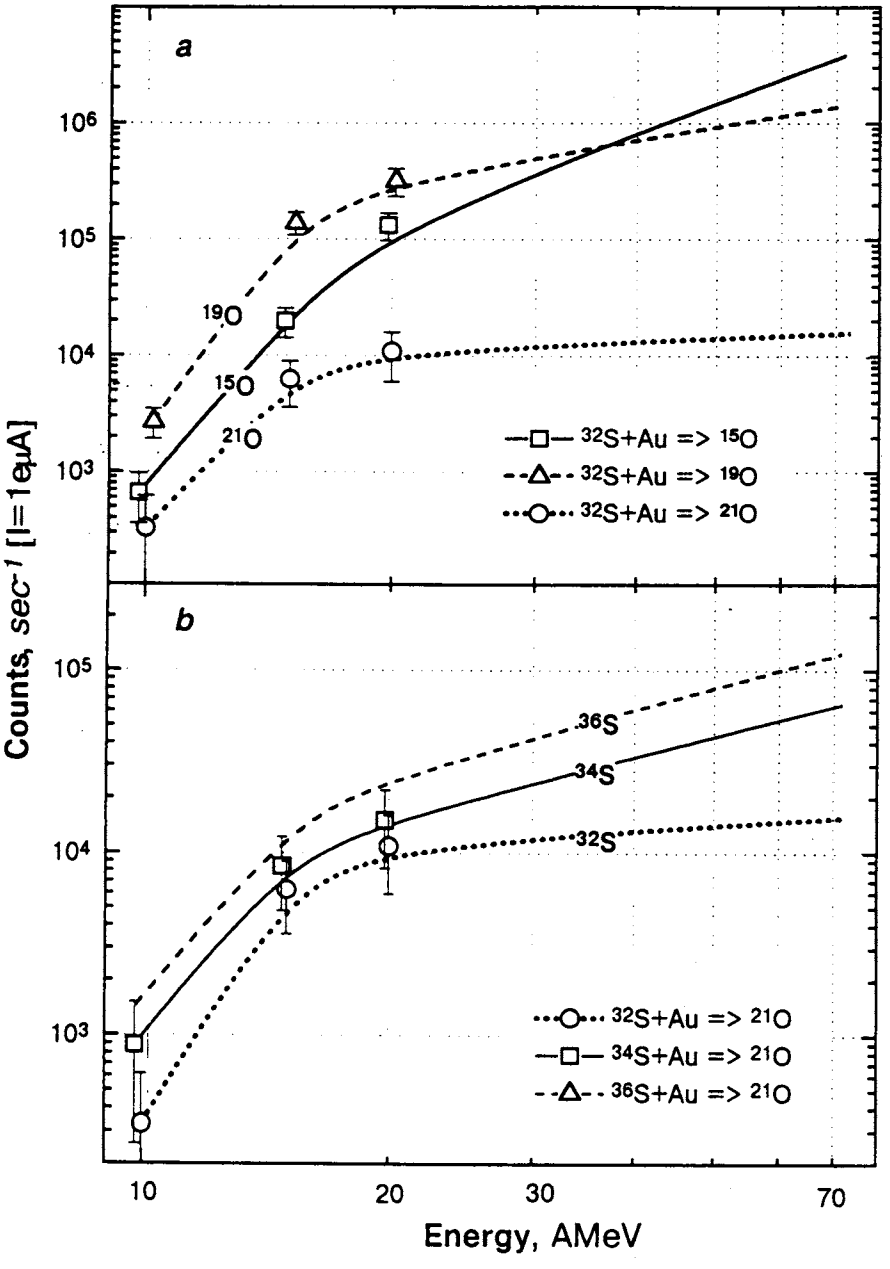

Fig.10. Yields of oxygen isotopes in S-induced reactions on a gold target at a beam current of 1 eμA vs projectile energy. (a) Yields of ^{15}O, ^{19}O, and ^{21}O in the case of a ^{32}S beam. (b) Yields of ^{21}O in the case of ^{32}S, ^{34}S, and ^{36}S beams. Calculations are performed assuming full absorption of the beam in the target

Taking into account that the intensity of the ^{32}S (20 MeV/A) beam in FLNR exceeds by an order of magnitude the intensity of the ^{36}S (75 MeV/A) beam at GANIL, one can expect comparative yields of neutron-rich isotopes within several mass units from the stability line for beams stopped in the target. However, for producing extremely neutron-rich nuclei with $12 \leq Z \leq 15$ the use of a ^{36}S beam is preferable (Fig.6d).

In addition, at it was mentioned earlier, the isotope production cross sections at energies $E < 20$ MeV/A depend on the energy of the reaction (Q_{gg}) and are highest for the smallest absolute values of Q_{gg} (Fig.7). The latter depend on the target-projectile combination and for the case presented in Fig.10 ($^{32}S + Au$) Q_{gg} is not the optimal one ($Q_{gg} < -50$ MeV) for deep inelastic reactions. The target can be chosen so as to have Q_{gg} equal to about – 30 MeV (e.g. Nb) and then the expected isotope yields may increase several times.

4. Conclusions

On the basis of the obtained data the following conclusions can be drawn:

- For the energy range 7 ÷ 10 MeV/A a quite abrupt decrease in cross section is observed for the light target when the number of transferred protons is increased. At high energies this difference decreases and at intermediate energies it is negligible.
- As far as the dependence of the isotope yields on the target is concerned, there is evidence that at small projectile energies in the case of the heavy target with a large ratio $N/Z = 1.49$, on the average a shift of the centers of gravity of the differential-cross-section distributions occurs in the direction of the neutron-rich region, and vice versa for the light target ($N/Z = 1$). At intermediate energies this peculiarity of the isotope yields practically vanishes.
- At small incident energies oscillations are observed in the centers-of-gravity distributions. These oscillations are smoothed with increasing the energy.
- At high energies the isotopic content of the projectile plays a dominant role for the production of nuclei close to the projectile ($Z \geq 12$), while at energies $E < 20$ MeV/A the production cross sections for the ^{32}S and ^{34}S beams are comparable. A difference in cross sections is observed only in the region of nuclei heavier than the projectile, where pick-up reactions prevail.
- The isotope production cross sections are seen to rise for energies up to about 15 ÷ 20 MeV/A, after which they either flatten or pass through a maximum and drop for energy regions where fragmentation is expected to prevail.

It is worthwhile noting that for the further investigation of the reaction mechanism it is very important to obtain new information on the yields of reaction products and their angular distributions using ^{32}S and ^{34}S beams in the energy range 30 ÷ 75 MeV/A and a ^{36}S beam at 10 ÷ 50 MeV/A.

Acknowledgements

The authors would like to express their gratitude to A.V.Belozerov for the help in carrying out the experiments, and to A.V.Antonenko and T.N.Shneidman for fruitful discussions.

The present work was carried out with the support of the Russian Foundation for Fundamental Research (RFFI) under grant No.96-02-17381a and of the Bulgarian Foundation for Scientific Research under grant No.F503.

References

1. Artukh A.G. et al. — Nucl. Phys., 1971, v.A176, p.284.
2. Volkov V.V. — Phys. Reports, 1978, v.44, p.93 and references therein; Volkov V.V.— Treatise on Heavy-Ion Science, v.8, p.101 (ed. D.Allan Bromley, Plenum Press, 1989) and references therein.
3. Norenberg W. — Phys. Lett., 1974, v.B52, p.289.
4. Symons T.J.M. et al. — Phys. Rev. Lett., 1979, v.42, p.40; Westfall G.D. et al. — Phys. Rev. Lett., 1979, v.43, p.1595.
5. Guillemaud-Mueller D. et al. — Z. Physik, 1989, v.A332, p.189.
6. Borrel V. et al. — Z. Physik, 1986, v.A324, p.205.
7. Pougheon F. et al. — Z. Physik, 1987, v.A327, p.17.
8. Lewitowicz M. et al. — Phys. Letters, 1994, v.B322, p.20.
9. Penionzhkevich Yu.E. — Phys. Part. Nucl., 1994, v.25, p.394.
10. Maidikov V.Z. et al. — Pribori i Tech. Expt, 1979, v.4, p.68.
11. Belozyorov A.V. et al. — JINR Preprint, P15-89-255, Dubna, 1989.
12. Tarasov O.B. et al. — JINR Rapid Communications, 1996, No.5[79]-96, p.59.
13. Anne R. et al. — NIM, 1987, v.A257, p.215.
14. Sümmerer K. et al. — Phys. Rev., 1990, v.C42, p.2546.
15. Adamian G.G. et al. — Phys. Part. Nucl., 1994, v.25, p.583.
16. Schmidt R., Toneev V., Woloshin G. — Nucl. Phys., 1978, v.A311, p.247.
17. Schmidt R., Toneev V. — Yad. Fizika, 1979, v.30, p.112.
18. Borrel V. et al. — Z. Physik, 1983, v.A314, p.191.
19. Barashenkov V.S., Toneev V.D. — High Energy Interaction of Particles and Nuclei with Atomic Nuclei, Moscow, 1972 (in Russian).

Received on Marth 3, 1997.